Available online at www.sciencedirect.com
ScienceDirect
Metabolism Clinical and Experimental 59 (2010) 1257–1267
Metabolism
Clinical and Experimental
www.metabolismjournal.com

Suppressed glucose metabolism in acinar cells might contribute to the development of exocrine pancreatic insufficiency in streptozotocin-induced diabetic mice

Junying Han[a], Ye Q. Liu[a,b,*]

[a]*The Research Institute for Children, Children's Hospital, New Orleans, Louisiana*
[b]*Department of Pediatrics, LSUHSC, New Orleans, Louisiana*

Received 14 October 2009; accepted 23 November 2009

Abstract

High prevalence of exocrine pancreatic insufficiency has been observed in diabetic patients. However, the underlying mechanisms are not well known. Reduced cytosolic Ca^{2+} signals in pancreatic acinar cells may contribute to lower digestive enzyme secretion. It is well known that adenosine triphosphate (ATP) regulates cytosolic Ca^{2+} signals in acinar cells; however, little is known as to whether diabetes impairs glucose metabolism that produces ATP in acinar cells. Streptozotocin (STZ)-induced diabetic C57BL/6 mouse model was used. Four weeks after being diabetic, pancreatic acinar cells were isolated; and amylase secretion and contents, glucose utilization and oxidation, the activities of several key enzymes for glucose metabolism, and ATP and nicotinamide adenine dinucleotide phosphate (reduced form) (NADPH) contents were determined. Compared with controls, diabetic mice had lower body weight. Cholecystokinin-8– and acetylcholine-stimulated amylase secretion was significantly impaired, and total amylase activity in acinar cells of STZ-diabetic mice was markedly reduced. Glucose utilization and oxidation were suppressed; measured enzyme activities for glucose metabolism and the ATP and NADPH contents were significantly reduced. These data indicate that glucose metabolism and ATP and NADPH productions are very important for maintaining acinar cell normal function. Reduction of ATP (reduces cytosolic Ca^{2+} signals) and NADPH (reduces cell capability for antioxidative stress) productions may contribute to the development of exocrine pancreatic insufficiency in STZ-diabetic mice.
© 2010 Elsevier Inc. All rights reserved.

1. Introduction

The exocrine pancreas secretes a juice that contains a number of digestive enzymes, bicarbonate, and an isotonic fluid to help digestion and assimilation of foodstuffs [1,2]. Exocrine secretion is regulated by the autonomic nervous system [3,4] and by 2 gut hormones, cholecystokinin (CCK) and secretin [5,6]. In diabetic patients including type 1 (insulin-dependent diabetes mellitus [IDDM]) and type 2 diabetes mellitus, the exocrine pancreas is unable to produce an adequate amount of digestive enzyme, especially amylase; this results in indigestion of carbohydrate and fat. This inadequacy is referred to as *exocrine pancreatic insufficiency*. A considerable proportion of diabetic patients have shown mild to moderate indigestion and impairment of enzyme secretion. The prevalence of exocrine pancreatic insufficiency in IDDM ranges between 40% and 80% in these patients, and overall pancreatic enzyme secretion was decreased [7-10]. Several direct and indirect function tests are available for assessment of pancreatic function in the patients with exocrine pancreatic insufficiency; but until today, it is difficult to diagnose mild impaired exocrine function clinically [11]. Serum amylase and lipase concentrations are valuable for the diagnosis in humans but not in animals. Trypsin-like immunoreactivity concentrations are of limited value for the diagnosis of cat pancreatitis [12]. The dog was diagnosed with exocrine pancreatic insufficiency based on markedly decreased serum levels of trypsin-like immunoreactivity [13].

The underlying cellular and molecular mechanisms that cause exocrine pancreatic insufficiency in diabetic patients are not well known. Several mechanisms have been proposed to explain this insufficiency including insensitivity

* Corresponding author. The Research Institute for Children, Children's Hospital, New Orleans, LA 70118. Tel.: +1 504 896 2794; fax: +1 504 896 2722.
E-mail address: yliu@chnola-research.org (Y.Q. Liu).

0026-0495/$ – see front matter © 2010 Elsevier Inc. All rights reserved.
doi:10.1016/j.metabol.2009.11.018

of pancreatic acinar cell receptors to CCK [14,15], magnesium deficiency [16], reduced gene expression for amylase [17], and a decrease in cytosolic free Ca^{2+} concentration [16,17]. Cytosolic Ca^{2+} signals are crucial for the control of fluid and enzyme secretion from exocrine glands. Calcium release through inositol (1,4,5)-trisphosphate receptors (InsP3Rs) is the primary signal driving digestive enzymes and fluid secretion from pancreatic acinar cells [18]. Binding of secretagogues to Gαq-coupled receptors on pancreatic acinar cells results in phospholipase C–induced production of InsP3 and a subsequent elevation of intracellular Ca^{2+} [19]. Adenosine triphosphate (ATP) modulates receptors InsP3R2 and InsP3R3 with dramatically different sensitivities and modes of action [20]. Depletion of ATP attenuated agonist-induced Ca^{2+} signals in pancreatic acinar cells [21]. Thereby, reduction of ATP in acinar cells would be an important mechanism causing exocrine pancreatic insufficiency.

The levels of free radical oxygen species (ROS) are high in diabetic individuals [22-24]. ROS are detrimental and toxic to cells and tissues as a result of injury to lipids, nucleic acids, and proteins, leading to loss of membrane function and increased permeability, DNA mutation, and cell death, forming nonflexible aged proteins in the cells [25]. It has been reported that enhanced oxidative stress in pancreatic acinar cells impairs DNA and induces apoptosis [26,27]. Apart from antioxidant enzymes including catalase [28] and superoxide dismutase [29], the cells are also equipped with many other enzymes in glucose metabolic pathways for anti-ROS such as cytosol malic enzyme 1 (ME) and glucose-6-phosphate dehydrogenase (G6PDH) that produce nicotinamide adenine dinucleotide phosphate (reduced form) (NADPH); and the latter has a function for lipids and fatty acids synthesis [30,31]and, importantly, for anti-ROS [32,33]. If glucose metabolism in pancreatic acinar cells is suppressed, reduced ATP production and decreased capability for anti-ROS would appear. This study was designed to test the hypothesis that impaired glucose metabolism and reduced anti-ROS enzymes in glucose metabolic pathways in acinar cells relate to exocrine pancreatic insufficiency in the mice with streptozotocin (STZ)-induced IDDM.

2. Materials and methods

2.1. Animals

Male C57BL/6 mice aged 7 to 12 weeks that were from Jackson Laboratory (Bar Harbor, ME) were used for this research, and this project was approved by our Institutional Animal Care and Use Committees. The principles of animal laboratory care under the guidelines of both NIH and the University of Louisville and Research Institute for Children's Institutional Animal Care and Use Committees were followed strictly. The mice (7 weeks old) were divided into 2 groups, 10 mice for each group. Group 2 was injected with STZ (180 mg/kg body weight, freshly dissolved in 5 mmol/L citrate buffer, pH 4.5) through jugular vein after anesthetization. Group 1 was injected with vehicle only for control. The mice in group 2 became diabetic (glucose levels, 350-450 mg/dL) about 3 days after STZ injection. If the values of blood glucose were less than 350 mg/dL or greater than 450 mg/dL, these mice were excluded from this project. All animals were fed a basal diet, and daily food consumption was determined. Body weight was recorded, and blood was collected after tail snipping. Blood glucose was measured using a glucose analyzer (Analox Instruments, Lunenburg, MA). The mice were maintained at 25°C with a 12-hour light/dark cycle. The mice were killed for exocrine isolation at the last day of week 4 after being diabetic.

2.2. Isolation of pancreatic acinar cells and protein content assay

After anesthetization, mouse pancreas was duct-infiltrated with 3 mL collagenase solution (1.5 mg/mL M199) and then isolated and incubated at 37°C for 18 minutes. After brief shaking and washing with M199 containing 10% fetal calf serum for 3 times, the digest was filtered through a 200-μm mesh (Sefar American, Depew, NY), followed by a brief centrifugation. The pellet was subjected to Ficoll density gradient centrifugation, and the acinar cell–enriched fraction was recovered as a pellet. The acinar cells were diluted with a secretion buffer. The secretion buffer contained 10 mmol/L HEPES, 128 mmol/L NaCl, 4.7 mmol/L KCl, 0.58 mmol/L $MgCl_2$, 0.55 mmol/L Na_2HPO_4, 1.27 mmol/L $CaCl_2$, 20 mmol/L glutamine, and 5.5 mmol/L glucose, bubbled with 95% O_2 plus 5% CO_2 for 30 minutes, followed by adding 1× amino acid solution, 0.2% bovine serum albumin (BSA), and 0.1 mg/mL soybean trypsin inhibitor. Cell viability detected using trypan blue was greater than 95%. The absence of mature pancreatic islets in this fraction was confirmed by dithizone staining [34]. Acinar cell protein was measured by a commercial kit that used BSA as standard (Bio-Rad, Hercules, CA).

2.3. Amylase secretion and activity assay

Tissue culture tubes (15 mL) containing acini were incubated with a secretion buffer described above for 1 hour at 37°C under constant O_2 with shaking (70 rpm); then the acini were stimulated with various concentrations of CCK-8 (10 pmol/L to 1 nmol/L) or acetylcholine (ACh) (10 nmol/L to 0.1 mmol/L) and continuously incubated and shaken for 30 minutes. The reaction was stopped by standing the tubes on the ice for 5 minutes and then centrifuged briefly at 4°C. Secreted amylase in the supernatants and total amylase activity in acinar cells in the pellets were measured. Protein contents in acinar cells were also determined. Amylase activity was measured using Phadebas Amylase Test (Magle, Lund, Sweden; batch no. 7M5018) and a spectrophotometer (U3310, Hitachi, Tokyo, Japan) according to the instruction.

2.4. Acinar cell glucose utilization and oxidation measurements

Glucose utilization was measured by the Ashcroft method [35]. Acinar cells (equal to 20 μg protein, duplicate) underwent a 30-minute preincubation in Krebs-Ringer buffer (KRB) containing 5.5 mmol/L glucose and trypsin inhibitor (0.1 mg/mL), followed by a 90-minute incubation at 37°C in 100 μL KRB containing glucose (5.5 or 16.7 mmol/L) plus 2 μCi D-[5-^{3}H]glucose (Amersham, Arlington Heights, IL) and trypsin inhibitor (0.1 mg/mL). The reaction took place in a 1-mL cup fit inside a rubber-stoppered 20-mL scintillation vial with 500 μL of distilled water surrounding the cup. Glucose utilization was stopped with 100 μL of 1 mol/L HCl injected through the stopper into the cup. After overnight incubation at 37°C to allow equilibration of the [^{3}H]H_2O in the reaction cup with the distilled water, the radioactivity in the distilled water was determined using a liquid scintillation counter. Tubes containing [^{3}H]H_2O and no acinar cells were used to estimate the recovery of [^{3}H]H_2O in the water, which was routinely close to 50%. Glucose oxidation was measured by the described method [36]. Acinar cells (20 μg protein, duplicate) were incubated for 90 minutes at 37°C in 100 μL KRB containing glucose (5.5 and 16.7 mmol/L), 1.7 μCi [U-^{14}C] glucose (NEN, Cambridge, MA), and trypsin inhibitor (0.1 mg/mL). The reaction was carried out in a 1-mL cup in a 20-mL scintillation vial capped by a rubber stopper with a center well that contained filter paper (Kontes, Vineland, NJ). Acinar cell glucose oxidation was stopped with 200 μL of 1 mol/L HCl injected through the stopper into the cup containing acinar cells. Liberated $^{14}CO_2$ was trapped in the filter paper in the center well by injecting 100 μL of 1 mol/L KOH into the filter paper, followed 2 hours later by liquid scintillation counting. Tubes containing [^{14}C] $NaHCO_3$ and no acinar cells were used to estimate the recovery of $^{14}CO_2$ in the filter paper, which was routinely close to 100%.

2.5. Phosphofructokinase activity assay

Phosphofructokinase (PFK) Vmax was measured as described [35]. Acinar cells (50 μg per 0.1 mL of extraction buffer) were sonicated on ice in 15 mmol/L K_2PO_4, pH 7.0, 100 mmol/L KCl, 2 mmol/L EDTA, 2 mmol/L phenylmethylsulfonyl fluoride, 0.2 mg/mL leupeptin, 50 μg/mL aprotinin, and 0.1 mg/mL soybean trypsin inhibitor, and then centrifuged at 12 000*g* for 15 minutes at 4°C. Supernatant (20 μL) was added to 1 mL of reaction buffer containing 50 mmol/L Tris/HCl, pH 8.0, 1 mmol/L EDTA, 2.5 mmol/L dithiothreitol, 2 mmol/L $MgCl_2$, 5 mmol/L ammonium sulfate, 0.1 mg/mL soybean trypsin inhibitor, 1 mmol/L ATP, 1 mmol/L fructose 6-P, 0.16 mmol/L nicotinamide adenine dinucleotide phosphate (NADH), 0.4 U/mL aldolase, and 2.4 U/mL triosephosphate isomerase–0.8 U/mL glycerophosphate dehydrogenase mixture in a quartz cuvette; and the NADH metabolized over 15 minutes was assessed by spectrophotometer at 340 nm. The PFK activity was calculated based on 1 μmol of fructose 1,6-P_2 = 2 μmol of NADH consumed.

2.6. Pyruvate carboxylase activity assay

Pyruvate carboxylase (PC) activity was measured according to the method of MacDonald et al [37]. Ten microliters of acinar cell homogenate (10 μg protein) was incubated in 40 μL reaction buffer (2 mmol/L Na_3-ATP, 2.5 mmol/L $NaHCO_3$, 10 mmol/L $MgCl_2$, 100 mmol/L KCl, 1 mmol/L dithiothreitol, 8 mmol/L pyruvate, 0.2 mmol/L acetyl–coenzyme A [CoA], 0.1 mg/mL trypsin inhibitor, and 2 μCi [^{14}C]$NaHCO_3$/mL) at 37°C for 30 minutes. The reaction was stopped by addition of 50 μL 10% trichloroacetic acid followed by overnight air drying and liquid scintillation counting.

2.7. Active pyruvate dehydrogenase activity assay

Active pyruvate dehydrogenase (PDH) assay was measured as described previously [36,38]. Acinar cells (100 μg protein) were homogenized on ice in 0.3 mL of 50 mmol/L HEPES, pH 7.5, 0.2 mmol/L KCl, 3 mmol/L EDTA, 5 mmol/L dithiothreitol, 0.1 mmol/L Na-*p*-tosyl-L-lysine chloromethyl ketone, 0.1 mmol/L trypsin inhibitor, 2% rat serum, and 0.25% (vol/vol) Triton X-100 and then freeze-thawed 3 times and passed through a 0.5-mL insulin syringe 10 times. Fifty microliters of acinar cell extract and 50 μL of reaction buffer (50 mmol/L HEPES, pH 7.5, 1 mmol/L $MgCl_2$, 3 mmol/L NAD, 0.4 mmol/L thiamine pyrophosphate, 0.4 mmol/L CoA, 2 mmol/L dithiothreitol, 0.1% Triton X-100, 7.5 U/mL lipoamide dehydrogenase, 0.1 mmol/L trypsin inhibitor, 1 mmol/L pyruvate, and 0.1 μCi of [1-^{14}C] pyruvate) were added to a cup inside a rubber-stoppered 20-mL scintillation vial that contained a center well with filter paper. After incubation at 37°C for 20 minutes, the reaction was stopped by injecting 200 μL of 1 mol/L HCl into the cup. $^{14}CO_2$ was trapped in the filter paper by injecting 100 μL of 1 mol/L KOH into the center well.

2.8. Cytosol malic enzyme 1 activity assay

Acinar cells were homogenized in a buffer containing 10 mmol/L HEPES, pH 7.4, 250 mmol/L sucrose, 2.5 mmol/L EDTA, 2 mmol/L cysteine, and 0.1 mg/mL BSA (wt/vol) and 0.1 mg/mL trypsin inhibitor. The homogenate was centrifuged at 10 000*g* for 15 minutes, and the supernatant was collected for ME activity and protein assays. All buffers before enzyme assay were kept cold on ice. Cell extract (50 μg protein) or NADPH standard (1-100 nmoL) was added to 1 mL of reaction buffer (50 mmol/L Tris/HCl, pH 7.8, 4 mmol/L $MgCl_2$, 0.1 mmol/L $NADP^+$, and 1 mmol/L malate). The change in fluorescence from 1 to 10 minutes was measured at room temperature at excitation of 340 nm and emission of 420 nm using a Hitachi F-2500 Fluorescence Spectrophotometer. Actual sample values were obtained by subtracting blank values (without cell extracts) from the sample values (with cell extracts).

2.9. Total RNA extraction from acinar cells, quantitative polymerase chain reaction, and real-time polymerase chain reaction

Acinar cells were put into a 1.5-mL RNase-free pellet pestle/homogenizing tube (Kontes Glass), and 600 μL RLT lysis buffer was added. The cells were homogenized by thoroughly grinding and centrifuged at 15 000*g* for 3 minutes. The cells were washed with PBS (Mg^{++} and Ca^{++} free) and digested for 10 minutes with 0.25% trypsin (Invitrogen, Carlsbad, CA), and then ice-cold RPMI 1640 (containing 10% newborn calf serum) was added to stop the digestion. The cells were transferred to a 10-mL sterile RNase-free tube and were washed and centrifuged 3 times at 300*g* at 4°C for 4 minutes. Total cellular RNA was isolated from acinar cells using an RNeasy Mini kit (Qiagen, Germantown, MD) according to protocol, and RNA concentration was determined using a RiboGreen RNA Quantization kit (Molecular Probes, Eugene, OR). Complementary DNA synthesis was carried out using Brilliant quantitative polymerase chain reaction (PCR) kit (Stratagene, La Jolla, CA) according to the manufacturer's protocol. Universal PCR Master Mix (Applied Biosystems, Carlsbad, CA) was diluted according to the manufacturer's procedure for quantitative PCR [39]. The final concentration of primer was 0.9 μmol/L, and the probe was 0.25 μmol/L. Relative copy numbers were calculated using the Pfaffl method [40]. The sequences designed for detecting *Me* gene expression by real-time-PCR in mouse acinar cells were as follows: forward (5′-3′), tgtgggaacagaaaatgaggagtt; reverse, tcatccaggaaggcgtcatact; probe, ccactgtacatcgggctgcggcac.

2.10. Glucose-6-phosphate dehydrogenase and 6-phosphogluconate dehydrogenase activity measurements

The activities of these 2 enzymes were measured in the supernatant of acinar cells (50 μg protein) that were sonicated in 20 mmol/L HEPES, pH 7.4, 50 mmol/L KCl, 0.5 mmol/L dithiothreitol, and 0.1 mg/mL trypsin inhibitor, and centrifuged at 14 000*g* for 10 minutes; 6- phosphogluconate dehydrogenase(6-PGDH) alone and total dehydrogenase activity (G6PDH plus 6-PPGDH) were measured according to a method previously described [41]. The G6PDH activity was calculated as the difference between the 6-PGDH activity and total dehydrogenase activity.

2.11. ATP measurement

Adenosine triphosphate content measurement was performed using a commercial kit (Molecular Probes).

2.12. NADPH and $NADP^+$ measurements

The NADPH or $NADP^+$ contents in acinar cell extract were measured by a modified method in our laboratory [42] based on a cycling method described by Lowry and Passonneau [43].

2.13. Statistical analysis

All data are expressed as means ± SE. The listed n values represent the number of a single experiment performed, and each single experiment was duplicated. Comparisons between 2 groups were performed by Student *t* test. Comparisons between multiple groups were performed by 1-way analysis of variance (Tukey post hoc test). A value of $P < .05$ was considered significant.

3. Results

3.1. Blood glucose levels, body weight, and food consumption in STZ-diabetic mice

Blood glucose levels, body weight gain, and food consumption in the mice are shown in Fig. 1. Fasted (3 hours) blood glucose levels (Fig. 1A) in STZ group were significantly increased and maintained at around 350 to 450 mg/dL. Fasted body weight (Fig. 1B) in STZ group was significantly lower than that in control group since week 1 after STZ injection. Daily food consumption (Fig. 1C) in diabetic group was significantly increased; this is different from humans. In humans, reduced food intake can be seen in many diabetic patients [7-10]. Despite increased food consumption, however, body weight in STZ-diabetic mice was significantly lower than that in control, suggesting that food indigestion or malabsorption occurred in diabetic mice.

3.2. Amylase secretion and synthesis in acinar cells

Because amylase accounts for 20% of total protein secreted by the pancreas [17], reduction of amylase secretion stimulated by CCK is usually used as a parameter of exocrine pancreatic insufficiency. As shown in Fig. 2A, basal amylase secretion (no CCK-8) in acinar cells was significantly reduced. Amylase secretion in response to CCK-8 stimulation was dramatically increased (10 to 100 pmol/L CCK-8) in control group; however, this response was significantly reduced in STZ-diabetic group, suggesting that acinar cell secretory function was impaired or that CCK receptors in acinar cells were desensitized by diabetes. To confirm this reduction, we used ACh to repeat amylase secretion. As shown in Fig. 2B, amylase secretion in response to ACh stimulation in STZ-diabetic group was similar to that in response to CCK-8. In addition, total amylase activity measured in acinar cells used for amylase secretion was also significantly reduced in diabetic mice (Fig. 2C), suggesting that amylase synthesis and/or enzyme activity was inhibited by diabetes.

3.3. Glucose utilization and glucose oxidation in acinar cells

Because glucose metabolism regulates ATP production, we measured [5-^{3}H]glucose utilization and [U-^{14}C]glucose oxidation in acinar cells isolated from these mice. As shown

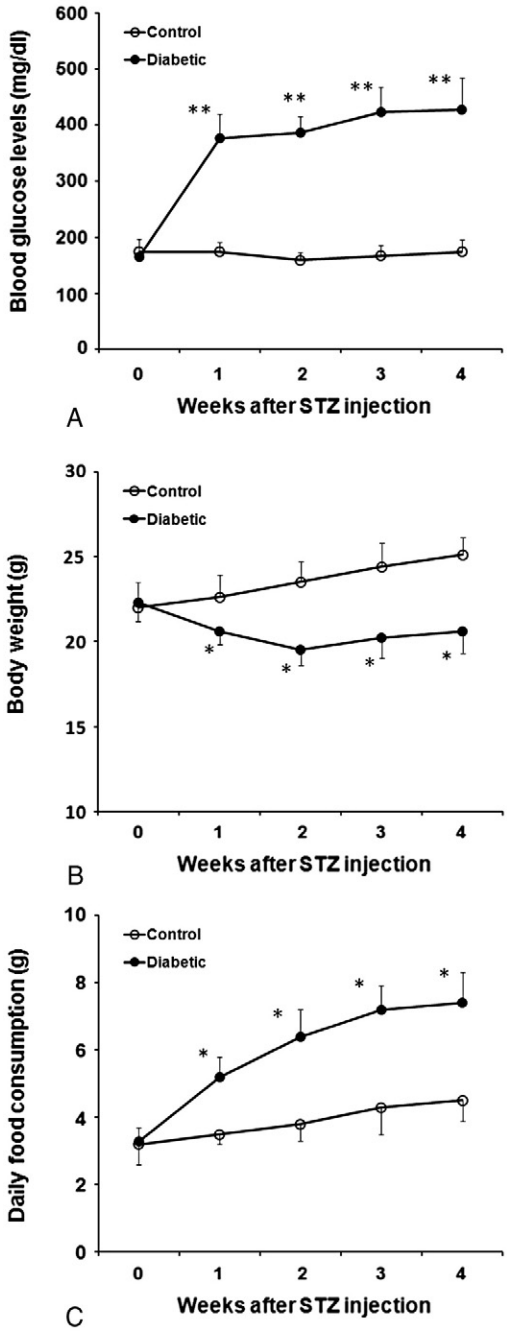

Fig. 1. Monitored blood glucose levels (A), body weight (B), and daily food consumption (C) in control and STZ-diabetic C57BL/6 mice. Seven-week-old C57BL/6 male mice were divided into 2 groups (control and diabetic groups), 10 mice for each group. Diabetic group was injected with STZ (180 mg/kg body weight, freshly dissolved in 5 mmol/L citrate buffer, pH 4.5) through jugular vein after anesthetization. Control group was injected with vehicle only. The STZ-injected mice became diabetic (glucose levels, 350-450 mg/dL) about 3 days after STZ injection. If the values of blood glucose were less than 350 mg/dL or greater than 450 mg/dL, these mice were excluded from this project. Values are mean ± SE. n = 10. $P < .05$, $^{**}P < .01$ between control and diabetic groups at each time point, respectively.

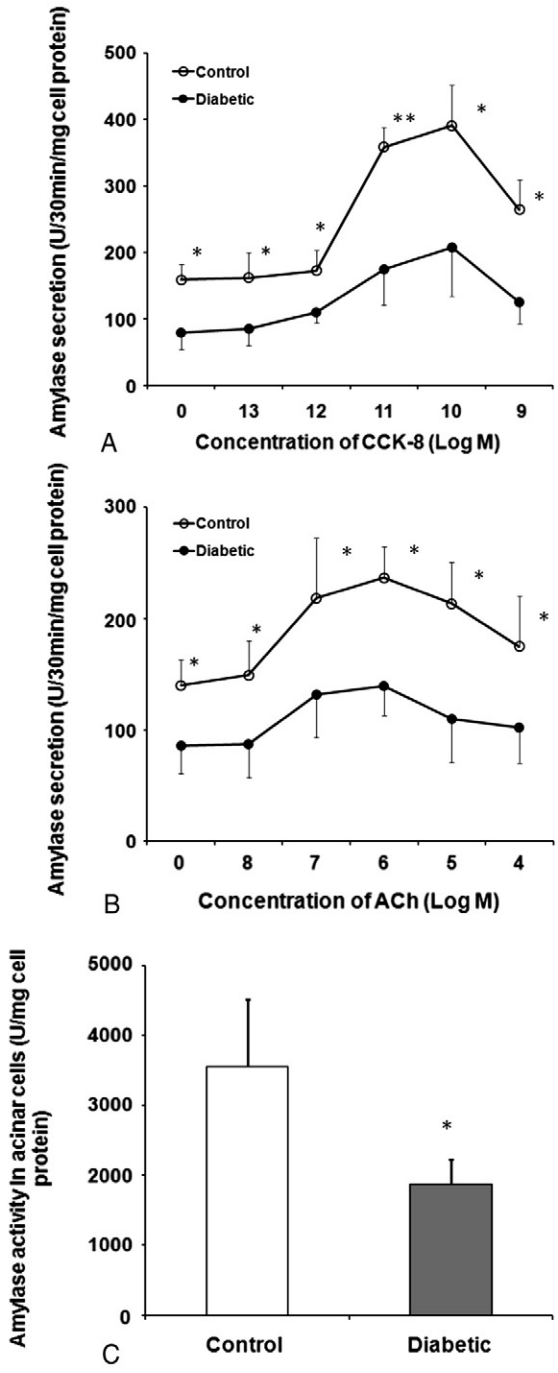

Fig. 2. Amylase secretion stimulated by CCK-8 (A) and ACh (B) and amylase activity in acinar cells (C) isolated from control and STZ-diabetic C57BL/6 mice. The methods for acinar cell isolation are described in the "Materials and methods" section. Cell viability detected using trypan blue was greater than 95%. The acini were stimulated with various concentrations of CCK-8 (10 pmol/L to 1 nmol/L) or ACh (10 nmol/L to 0.1 mmol/L) and continuously incubated and shaken for 30 minutes. The reaction was stopped by standing the tubes on ice for 5 minutes and then centrifuged briefly at 4°C. Secreted amylase in the supernatants and total amylase activity in acinar cells in the pellets were measured using Phadebas Amylase Test. Values are mean ± SE. n = 6. $P < .05$, $^{**}P < .01$ between control and diabetic groups at each time point, respectively.

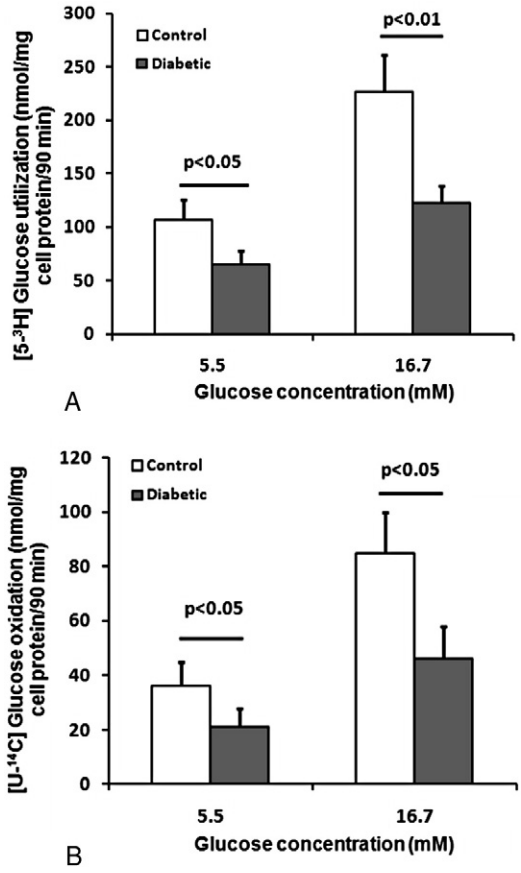

Fig. 3. [5-^{3}H]Glucose utilization (A) and [U-^{14}C]glucose oxidation (B) in acinar cells isolated from control and STZ-diabetic C57BL/6 mice. Acinar cells (equal to 20 μg protein, duplicate) underwent a 30-minute preincubation in KRB containing 5.5 mmol/L glucose and trypsin inhibitor (0.1 mg/mL), followed by a 90-minute incubation at 37°C in 100 μL KRB containing glucose (5.5 or 16.7 mmol/L) plus 2 μCi D-[5-^{3}H]glucose or 1.7 μCi [U-^{14}C] glucose and trypsin inhibitor (0.1 mg/mL). Released [^{3}H]H_2O or $^{14}CO_2$ were trapped and then counted by a scintillation counter. Values are mean ± SE. n = 4.

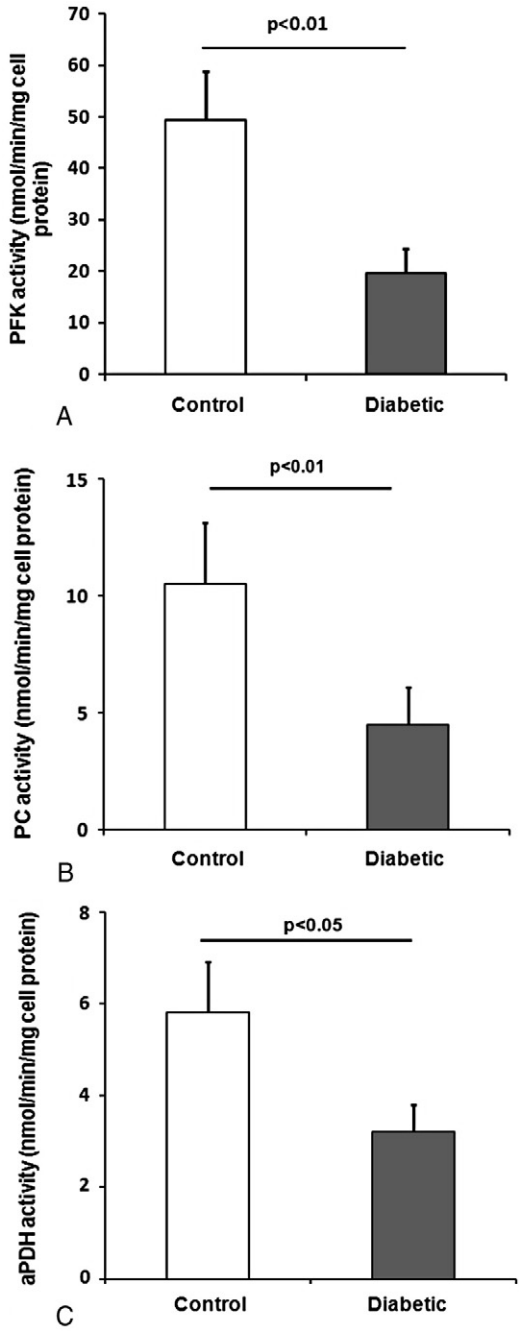

Fig. 4. Phosphofructokinase (A), PC (B), and active PDH (C) activities in acinar cells isolated from control and STZ-diabetic C57BL/6 mice. Acinar cells were sonicated in the buffers; PFK and PC activities were measured using an enzymatic (PFK) or isotope tracer method described in the "Materials and methods" section. Values are mean ± SE. n = 6.

in Fig. 3, both glucose utilization and oxidation were significantly reduced in the acinar cells of STZ-diabetic mice. Basal glucose metabolism measured at 5.5 mmol/L glucose in diabetic group was also significantly reduced. These data were consistent with the changes in basal amylase secretion (Fig. 2), suggesting that glucose metabolism also regulates basal amylase secretion.

3.4. Glucose metabolic enzyme activities in acinar cells

To better understand the significant reduction in glucose utilization and oxidation and amylase secretion, we measured some key metabolic enzyme activities in acinar cells of control and STZ-diabetic mice. Phosphofructokinase [44] controls glucose utilization, PC [45], and PDH [46] metabolize pyruvate derived from glucose into the tricarboxylic acid cycle, govern glucose oxidation. As shown in Fig. 4, the activities of these 3 enzymes in acinar cell were significantly reduced in STZ-diabetic group. These changes are consistent with impaired glucose utilization and oxidation in diabetic acinar cells (Fig. 3).

3.5. NADPH-producing enzyme activities and Me mRNA expression levels in acinar cells

NADPH has a function for anti-ROS [32,33]. NADPH is produced by the pentose phosphate pathway (PPP) [47] and other NADPH-producing enzymes including ME [48].

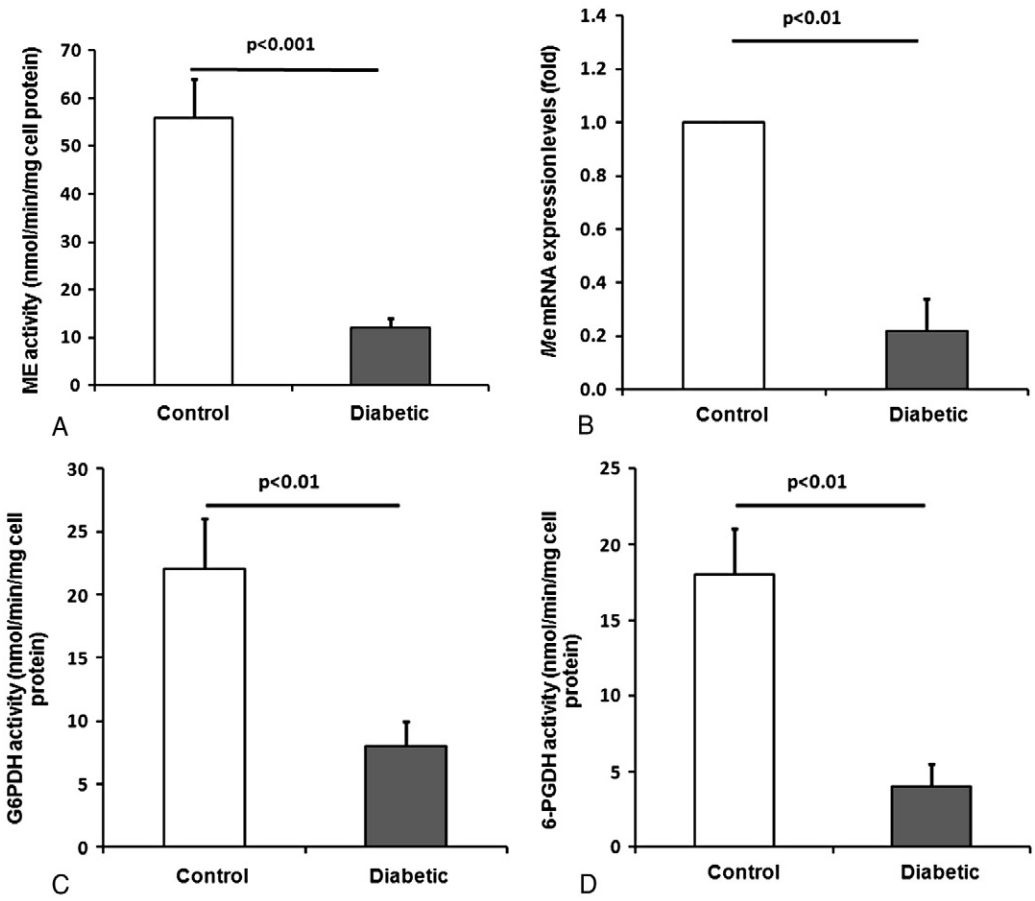

Fig. 5. Cytosol malic enzyme 1 (A), G6PDH (C), and 6-PGDH (D) activities and *Me* mRNA expression levels (B) in acinar cells isolated from control and STZ-diabetic C57BL/6 mice. *Me* activity was measured using a fluorometer at room temperature at excitation of 340 nm and emission of 420 nm. *Me* mRNA expression levels were measured by real-time-PCR. 6-Phosphogluconate dehydrogenase alone and total dehydrogenase activity (G6PDH plus 6-PPGDH) were measured separately, and G6PDH activity was calculated as the difference between the 6-PGDH activity and total dehydrogenase activity. Values are mean ± SE. n = 6.

Glucose-6-phosphate dehydrogenase and 6-PGDH are 2 key enzymes to produce NADPH in PPP. Cytosol malic enzyme 1 is located in pyruvate cycling [49,50] and pyruvate-citrate cycle [51,52]. These 2 cycles have been identified in pancreatic β-cells but not in acinar cells. As shown in Fig. 5A, C, and D, the activities of these 3 enzymes were significantly reduced in diabetic acinar cells, suggesting that (1) pyruvate cycling and pyruvate-citrate cycle might exist in the acinar cells because of measurable ME activity and (2) NADPH production may be reduced in diabetic acinar cells. To further support our findings of ME activity in diabetic acinar cells, we measured *Me* mRNA by Taqman real-time PCR. As shown in Fig. 5B, *Me* mRNA expression levels in diabetic acinar cells were about 21% of control group. This percentage of *Me* mRNA level in diabetic acinar cells compared to control is similar to that in enzyme activity level (14%, Fig. 5A).

3.6. ATP contents and NADPH/NADP$^+$ ratios in acinar cells

Because glucose metabolism and enzyme activities in metabolic pathways were significantly reduced, we measured ATP, NADPH, and NADP$^+$ contents in diabetic acinar cells. As shown in Fig. 6A, as expected, ATP contents in diabetic acinar cells were significantly reduced, consistent with reduced glucose metabolism. The NADPH/NADP$^+$ ratios in response to high (16.7 mmol/L) glucose were significantly ($P < .01$) increased in control group (Fig. 6B). In diabetic group, the NADPH/NADP$^+$ ratios in response to high glucose were also significantly increased; but this increase was lower than that in control ($P < .05$). Importantly, both basal (2.8 mmol/L glucose)– and high glucose–stimulated NADPH/NADP$^+$ ratios were reduced in diabetic group, consistent with reduced glucose oxidation and enzyme activities in glucose oxidation pathways and PPP.

4. Discussion

Exocrine pancreatic insufficiency in diabetic patients has been known for a long time; but the mechanisms causing this insufficiency are not well known, and the decrease in cytosolic free Ca^{2+} concentration in diabetic acinar cells is proposed to be an important causal mechanism [16,17]. In response to CCK or ACh, the secretory process has been

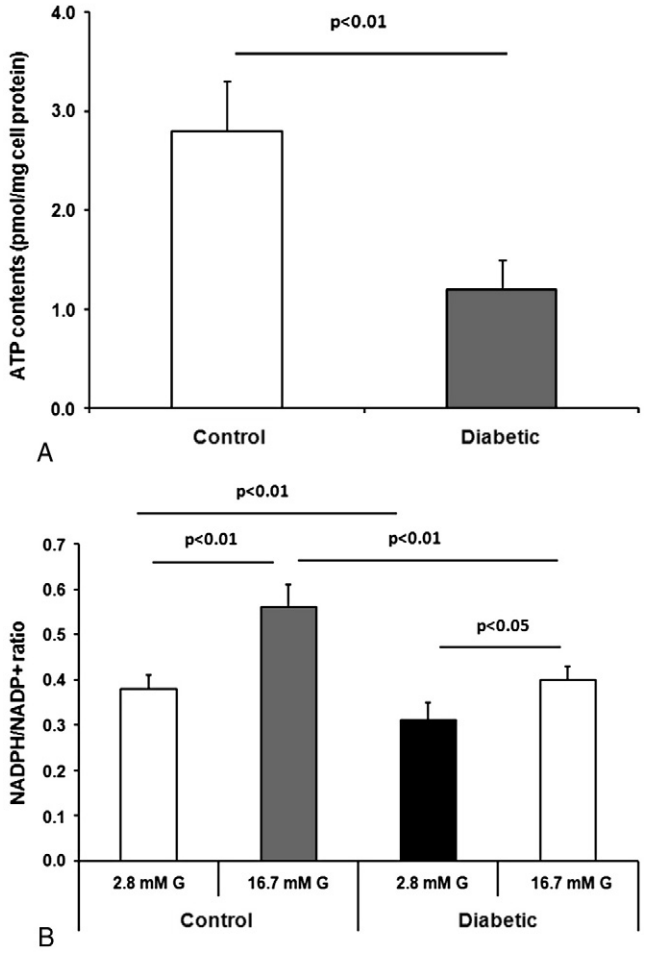

Fig. 6. Adenosine triphosphate contents (A) and NADPH/NADP$^+$ ratios (B) in acinar cells isolated from control and STZ-diabetic C57BL/6 mice. Adenosine triphosphate content measurement was performed using a commercial kit (Molecular Probes); NADPH or NADP$^+$ contents in acinar cell extract were measured by a modified enzymatic cycling method. Values are mean ± SE. n = 4.G indicates glucose.

shown to be highly dependent upon the presence of extracellular Ca^{2+} [16,53]. As described in the "Introduction" section, ATP plays a key role in the elevation of cytosolic Ca^{2+} signals through InsP3Rs; and enhanced cytosolic Ca^{2+} signals promote enzyme secretion. Therefore, reduction of ATP in acinar cells would be an important mechanism causing exocrine pancreatic insufficiency. Normal glucose metabolism would be very important for producing enough ATP for enzyme secretion from the acinar cells. Current studies determined glucose metabolism in acinar cells of STZ-induced diabetic mice. Our data demonstrated that glucose utilization and oxidation, enzyme (PFK, PC, and PDH) activities in glucose metabolic pathways, and ATP production were significantly reduced. Reduced glucose metabolism is consistent with suppressed amylase secretion, implying that glucose metabolism regulates amylase secretion. These data support the hypothesis that glucose metabolism and ATP production play key roles in the regulation of amylase secretion from acinar cells.

Many enzymes have to work together to complete glucose utilization and oxidation. In this study, we chose PFK as a representative enzyme for glucose utilization, and PC and PDH for glucose oxidation, respectively. Phosphofructokinase is located in the cytosol and converts fructose 6-phosphate into fructose 1,6-bisphosphate [44]. Pyruvate carboxylase is located in the mitochondria and converts carbons from pyruvate derived from glucose into the tricarboxylic acid cycle intermediate oxaloacetate [37,54]. Pyruvate is also catalyzed into acetyl-CoA in the mitochondria by PDH [38,55]. Adenosine triphosphate is produced by both glycolysis and glucose oxidation (most ATP is produced by oxidation); thus, it is very easy to understand that the reduction of glucose utilization and oxidation results in reduced ATP production. Increased ROS in diabetes may be the key factor to inhibit metabolic enzyme activities. Phosphofructokinase and other enzyme activities in glycolytic pathway were significantly reduced in diabetic livers [56,57]; PC [37,54] and PDH [38,55] activities were inhibited in diabetic islets. Our data demonstrated that glucose utilization and oxidation in acinar cells were suppressed by frank diabetes.

It is well known that ROS levels are significantly increased in diabetes [22–24]. Free radical oxygen species is the radical form of oxygen. Free radical oxygen species is a normal byproduct of mitochondrial respiration and enzymatic oxidases [58]. Free radical oxygen species is capable of acting as signaling molecules, but also causes damage to cellular proteins, lipids, and nucleic acids [59]. The putative role of ROS in the development of diabetic complications has been investigated for several decades [25,60,61]. Oxidative stress plays critical roles in the pathogenesis of various diseases [62]. In the diabetic condition, oxidative stress impairs glucose transport and glucose uptake in muscle and fat [63,64] and reduces anti-ROS enzyme activities in brain [65]; but whether diabetes reduces anti-ROS enzyme activities in pancreatic acinar cells is not well known. NADPH plays an important role in wiping out ROS [32,33]. NADPH is produced by at least 2 cycles or pathways. One is pyruvate cycling; the other is PPP. Pyruvate cycling produces significantly more NADPH than the PPP in the β-cells [66]. Cytosol malic enzyme 1 is located in not only pyruvate cycling [49,50] but also pyruvate-citrate cycle [51,52] in β-cells. Cytosol malic enzyme 1 is known to play a significant role in insulin secretion in pancreatic β-cells [67,68]. Pyruvate cycling and pyruvate-citrate cycle have not been identified in acinar cells yet. Therefore, whether these 2 cycles regulate amylase secretion is completely unknown; and how much percentage of NADPH is produced by PPP or by pyruvate cycling is also unknown. Because ME activity and *Me* mRNA can be measured in acinar cells, and both ME activity and *Me* mRNA expression levels are significantly reduced in diabetic acinar cells; these suggest that pyruvate cycling and pyruvate-citrate cycle might exist in exocrine

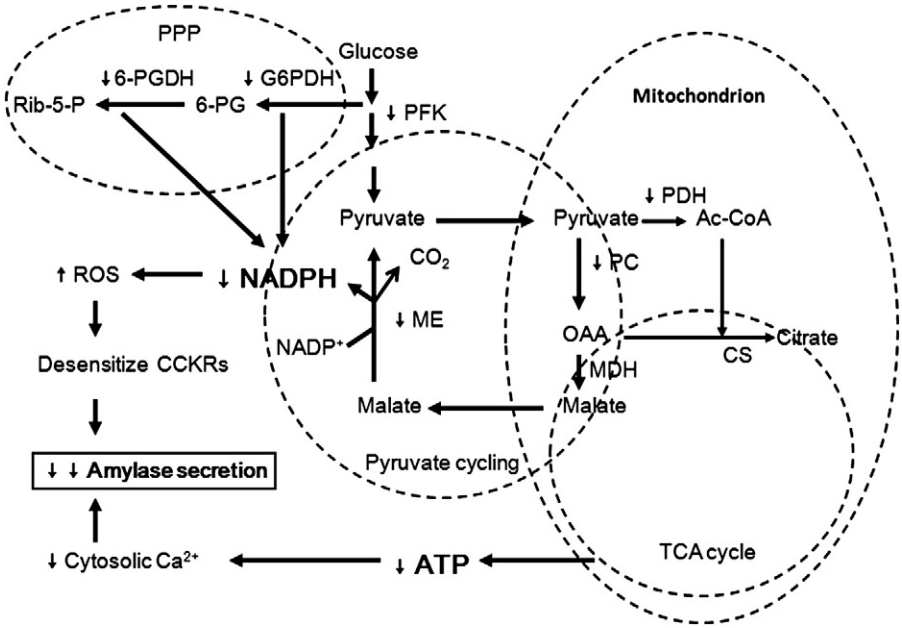

Fig. 7. Proposed metabolic scheme for explaining how reduced glucose metabolism inhibits amylase secretion in acinar cells in diabetic mice. Reduced glucose utilization and oxidation lead to a reduction in ATP production; the latter decreases cytosolic free Ca^{2+} concentrations, leading to impaired amylase secretion. Reduced enzyme activities of ME, G6PDH, and 6-PGDH lead to reduction of NADPH production; the latter makes the acinar cells vulnerable to increased ROS, leading to CCK receptor insensitivity. We propose that these 2 major changes in acinar cells contribute to the development of exocrine pancreatic insufficiency in diabetic mice. ↑ means increase; ↓ means decrease. Ac-CoA indicates acetyl–CoA; CCKRs, CCK receptors; CS, citrate synthase; MDH, malate dehydrogenase; OAA, oxaloacetate.

cells. Because ME produces NADPH, we hypothesize that ME plays an important role in anti-ROS in acinar cells; reduced ME activity would decrease the capability of acinar cells for anti-ROS. Glucose-6-phosphate dehydrogenase and 6-PGDH can also produce NADPH. Thus, these 2 enzymes may play a similar role as ME does in acinar cells; and these 2 enzymes' activities were markedly reduced in diabetic group. Reduced activities of ME, G6PDH, and 6-PGDH would make diabetic acinar cells more sensitive to increased ROS.

Cholecystokinin- or ACh-stimulated amylase secretion was significantly reduced in the acinar cells (Fig. 2A), indicating that insensitivity of CCK or ACh receptors was significant. Because ROS levels are significantly increased in diabetes, ROS damage to the cells is multiple and severe [25], and attenuated anti-ROS system is observed, insensitivity of CCK and ACh receptors observed in diabetic acinar cells may be caused by ROS. However, enzyme secretion from the acinar cells is determined by not only receptor sensitivity but also its downstream signals such as Ca^{2+} that is regulated by ATP. Therefore, we propose that both reduced ATP and NADPH productions and increased ROS levels contribute to impaired amylase secretion.

5. Conclusion

In summary, our results have demonstrated that diabetes causes many metabolic aberrations in exocrine acinar cells that lead to a decrease in ATP and NADPH contents. We hypothesize (Fig. 7) that reduction of ATP decreases cyclic Ca^{2+} signals, leading to impaired amylase secretion; and reduced NADPH content makes the acinar cells more vulnerable to ROS damage, leading to CCK receptor insensitivity. These metabolic aberrations might be some of the mechanisms causing exocrine pancreatic insufficiency in STZ-induced diabetic mice.

Acknowledgment

This work was supported by a grant from the National Institutes of Health (1R01 DK077624-01). This project was also supported by a grant (6931) from the Research Institute for Children, Children's Hospital at New Orleans.

References

[1] Petersen OH, Ueda N. Secretion of fluid and amylase in the perfused rat pancreas. J Physiol 1977;264:819-35.
[2] Petersen OH. Stimulus-secretion coupling: cytoplasmic calcium signals and the control of ion channels in exocrine acinar cells. J Physiol 1992;448:1-51.
[3] Kiba T. Relationships between the autonomic nervous system and the pancreas including regulation of regeneration and apoptosis: recent developments. Pancreas 2004;29:e51-8.
[4] Konturek SJ, Zabielski R, Konturek JW, et al. Neuroendocrinology of the pancreas; role of brain-gut axis in pancreatic secretion. EurJ Pharmacol 2003;481:1-14.
[5] Yamamoto M, Shirohara H, Otsuki M. CCK-, secretin-, and cholinergic-independent pancreatic fluid hypersecretion in protease inhibitor-treated rats. Am J Physiol 1998;274:G406-12.

[6] Sabbatini ME, Rodriguez MR, Corbo NS, et al. C-type natriuretic peptide applied to the brain enhances exocrine pancreatic secretion through a vagal pathway. Eur J Pharmacol 2005;524:67-74.
[7] Hardt PD, Krauss A, Bretz L, et al. Pancreatic exocrine function in patients with type 1 and type 2 diabetes mellitus. Acta Diabetol 2000; 37:105-10.
[8] Rathmann W, Haastert B, Icks A, et al. Low faecal elastase 1 concentrations in type 2 diabetes mellitus. Scand J Gastroenterol 2001; 36:1056-61.
[9] Hussain K, Padidela R, Kapoor RR, et al. Diabetes mellitus, exocrine pancreatic deficiency, hypertrichosis, hyperpigmentation, and chronic inflammation: confirmation of a syndrome. Pediatr Diabetes 2008.
[10] Nunes AC, Pontes JM, Rosa A, et al. Screening for pancreatic exocrine insufficiency in patients with diabetes mellitus. Am J Gastroenterol 2003;98:2672-5.
[11] Keller J, Aghdassi AA, Lerch MM, et al. Tests of pancreatic exocrine function—clinical significance in pancreatic and non-pancreatic disorders. Best Pract Res Clin Gastroenterol 2009;23:425-39.
[12] Xenoulis PG, Steiner JM. Current concepts in feline pancreatitis. Top Companion Anim Med 2008;23:185-92.
[13] Chapman S, Thompson C, Wilcox A, et al. What is your diagnosis? Rectal scraping from a dog with diarrhea. Vet Clin Pathol 2009;38: 59-62.
[14] Otsuki M, Akiyama T, Shirohara H, et al. Loss of sensitivity to cholecystokinin stimulation of isolated pancreatic acini from genetically diabetic rats. Am J Physiol 1995;268:E531-6.
[15] Akiyama T, Otsuki M. Characterization of a new cholecystokinin receptor antagonist FK480 in in vitro isolated rat pancreatic acini. Pancreas 1994;9:324-31.
[16] Patel R, Yago MD, Manas M, et al. Mechanism of exocrine pancreatic insufficiency in streptozotocin-induced diabetes mellitus in rat: effect of cholecystokinin-octapeptide. Mol Cell Biochem 2004;261:83-9.
[17] Patel R, Shervington A, Pariente JA, et al. Mechanism of exocrine pancreatic insufficiency in streptozotocin-induced type 1 diabetes mellitus. Ann N Y Acad Sci 2006;1084:71-88.
[18] Ashby MC, Tepikin AV. Polarized calcium and calmodulin signaling in secretory epithelia. Physiol Rev 2002;82:701-34.
[19] Betzenhauser MJ, Wagner LE, Iwai M, et al. ATP modulation of Ca2+ release by type-2 and type-3 inositol (1, 4, 5)-triphosphate receptors. Differing ATP sensitivities and molecular determinants of action. J Biol Chem 2008;283:21579-87.
[20] Betzenhauser MJ, Wagner LE, Won JH, et al. Studying isoform-specific inositol 1,4,5-trisphosphate receptor function and regulation. Methods 2008;46:177-82.
[21] Park HS, Betzenhauser MJ, Won JH, et al. The type 2 inositol (1,4,5)-trisphosphate (InsP3) receptor determines the sensitivity of InsP3-induced Ca2+ release to ATP in pancreatic acinar cells. J Biol Chem 2008;283:26081-8.
[22] Ceriello A, Mercuri F, Quagliaro L, et al. Detection of nitrotyrosine in the diabetic plasma: evidence of oxidative stress. Diabetologia 2001; 44:834-8.
[23] Mercuri F, Quagliaro L, Ceriello A. Oxidative stress evaluation in diabetes. Diabetes Technol Ther 2000;2:589-600.
[24] Ceriello A, Morocutti A, Mercuri F, et al. Defective intracellular antioxidant enzyme production in type 1 diabetic patients with nephropathy. Diabetes 2000;49:2170-7.
[25] Oberley LW. Free radicals and diabetes. Free Radic Biol Med 1988;5: 113-24.
[26] Song JY, Lim JW, Kim H, et al. Oxidative stress induces nuclear loss of DNA repair proteins Ku70 and Ku80 and apoptosis in pancreatic acinar AR42J cells. J Biol Chem 2003;278:36676-87.
[27] Song JY, Lim JW, Kim H, et al. Role of NF-kappaB and DNA repair protein Ku on apoptosis in pancreatic acinar cells. Ann N Y Acad Sci 2003;1010:259-63.
[28] Li X, Chen H, Epstein PN. Metallothionein and catalase sensitize to diabetes in nonobese diabetic mice: reactive oxygen species may have a protective role in pancreatic {beta}-cells. Diabetes 2006;55:1592-604.
[29] Valko M, Rhodes CJ, Moncol J, et al. Free radicals, metals and antioxidants in oxidative stress-induced cancer. Chem Biol Interact 2006;160:1-40.
[30] Infante JP, Huszagh VA. Analysis of the putative role of 24-carbon polyunsaturated fatty acids in the biosynthesis of docosapentaenoic (22:5n-6) and docosahexaenoic (22:6n-3) acids. FEBS Lett 1998; 431:1-6.
[31] Dmitriev LF. Activity of key enzymes in microsomal and mitochondrial membranes depends on the redox reactions involving lipid radicals. Membr Cell Biol 2001;14:649-62.
[32] Furukawa S, Fujita T, Shimabukuro M, et al. Increased oxidative stress in obesity and its impact on metabolic syndrome. J Clin Invest 2004; 114:1752-61.
[33] Rydstrom J. Mitochondrial NADPH, transhydrogenase and disease. Biochim Biophys Acta 2006;1757:721-6.
[34] Shiroi A, Yoshikawa M, Yokota H, et al. Identification of insulin-producing cells derived from embryonic stem cells by zinc-chelating dithizone. Stem Cells 2002;20:284-92.
[35] Liu YQ, Tornheim K, Leahy JL. Fatty acid-induced beta cell hypersensitivity to glucose. Increased phosphofructokinase activity and lowered glucose-6-phosphate content. J Clin Invest 1998;101: 1870-5.
[36] Liu YQ, Tornheim K, Leahy JL. Glucose-fatty acid cycle to inhibit glucose utilization and oxidation is not operative in fatty acid-cultured islets. Diabetes 1999;48:1747-53.
[37] Macdonald MJ, Tang J, Polonsky KS. Low mitochondrial glycerol phosphate dehydrogenase and pyruvate carboxylase in pancreatic islets of Zucker diabetic fatty rats. Diabetes 1996;45:1626-30.
[38] Zhou YP, Ostenson CG, Ling ZC, et al. Deficiency of pyruvate dehydrogenase activity in pancreatic islets of diabetic GK rats. Endocrinology 1995;136:3546-51.
[39] Xu J, Han J, Epstein PN, et al. Regulation of PDK mRNA by high fatty acid and glucose in pancreatic islets. Biochem Biophys Res Commun 2006;344:827-33.
[40] Pfaffl MW. A new mathematical model for relative quantification in real-time RT-PCR. Nucleic Acids Res 2001;e45:29.
[41] Tian WN, Braunstein LD, Pang J, et al. Importance of glucose-6-phosphate dehydrogenase activity for cell growth. J Biol Chem 1998; 273:10609-17.
[42] Xu J, Han J, Long YS, et al. The role of pyruvate carboxylase in insulin secretion and proliferation in rat pancreatic beta cells. Diabetologia 2008;51:2022-30.
[43] Lowry OH, Passonneau JV. Enzymatic cycling. In: Lowry OH, Passonneau JV, editors. A flexible system of enzymatic analysis. New York: Academic Press; 1972. p. 129-45.
[44] Dunaway GA, Kasten TP. Nature of the subunits of the 6-phosphofructo-1-kinase isoenzymes from rat tissues. Biochem J 1987;242:667-71.
[45] Davis EJ, Spydevold O, Bremer J. Pyruvate carboxylase and propionyl-CoA carboxylase as anaplerotic enzymes in skeletal muscle mitochondria. Eur J Biochem 1980;110:255-62.
[46] Eboli ML. Pyruvate dehydrogenase levels in Morris hepatomas with different growth rate. Cancer Lett 1985;26:185-90.
[47] Sabate L, Franco R, Canela EI, et al. A model of the pentose phosphate pathway in rat liver cells. Mol Cell Biochem 1995;142:9-17.
[48] Macdonald MJ. Differences between mouse and rat pancreatic islets: succinate responsiveness, malic enzyme, and anaplerosis. Am J Physiol Endocrinol Metab 2002;283:E302-E310.
[49] Lu D, Mulder H, Zhao P, et al. 13C NMR isotopomer analysis reveals a connection between pyruvate cycling and glucose-stimulated insulin secretion (GSIS). Proc Natl Acad Sci U S A 2002;99:2708-13.
[50] Cline GW, LePine RL, Papas KK, et al. 13C NMR isotopomer analysis of anaplerotic pathways in INS-1 cells. J Biol Chem 2004;279: 44370-5.
[51] Macdonald MJ, Fahien LA, Brown LJ, et al. Perspective: emerging evidence for signaling roles of mitochondrial anaplerotic products in insulin secretion. Am J Physiol Endocrinol Metab 2005;288:E1-E15.

[52] Guay C, Madiraju SR, Aumais A, et al. A role for ATP-citrate lyase, malic enzyme, and pyruvate/citrate cycling in glucose-induced insulin secretion. J Biol Chem 2007;282:35657-65.
[53] Francis LP, Lennard R, Singh J. Mechanism of action of magnesium on acetylcholine-evoked secretory responses in isolated rat pancreas. Exp Physiol 1990;75:669-80.
[54] Macdonald MJ, Efendic S, Ostenson CG. Normalization by insulin treatment of low mitochondrial glycerol phosphate dehydrogenase and pyruvate carboxylase in pancreatic islets of the GK rat. Diabetes 1996; 45:886-90.
[55] Zhou YP, Berggren PO, Grill V. A fatty acid-induced decrease in pyruvate dehydrogenase activity is an important determinant of beta-cell dysfunction in the obese diabetic db/db mouse. Diabetes 1996;45: 580-6.
[56] Sochor M, Kunjara S, Baquer NZ, et al. Regulation of glucose metabolism in livers and kidneys of NOD mice. Diabetes 1991;40: 1467-71.
[57] Marcus F, Chatterjee T. Mouse (C57BL/KsJ) liver phosphofructokinase. Allosteric kinetics and age-related changes in the genetically diabetic state. J Biol Chem 1981;256:378-81.
[58] Yu BP. Cellular defenses against damage from reactive oxygen species. Physiol Rev 1994;74:139-62.
[59] Houstis N, Rosen ED, Lander ES. Reactive oxygen species have a causal role in multiple forms of insulin resistance. Nature 2006;440: 944-8.
[60] Baynes JW. Role of oxidative stress in development of complications in diabetes. Diabetes 1991;40:405-12.
[61] Baynes JW, Thorpe SR. Role of oxidative stress in diabetic complications: a new perspective on an old paradigm. Diabetes 1999;48:1-9.
[62] Brownlee M. Biochemistry and molecular cell biology of diabetic complications. Nature 2001;414:813-20.
[63] Maddux BA, See W, Lawrence Jr JC, et al. Protection against oxidative stress–induced insulin resistance in rat L6 muscle cells by micromolar concentrations of alpha-lipoic acid. Diabetes 2001;50:404-10.
[64] Rudich A, Tirosh A, Potashnik R, et al. Prolonged oxidative stress impairs insulin-induced GLUT4 translocation in 3T3-L1 adipocytes. Diabetes 1998;47:1562-9.
[65] Nakhaee A, Bokaeian M, Akbarzadeh A, et al. Sodium tungstate attenuate oxidative stress in brain tissue of streptozotocin-induced diabetic rats. Biol Trace Elem Res 2009.
[66] Macdonald MJ. Feasibility of a mitochondrial pyruvate malate shuttle in pancreatic islets. Further implication of cytosolic NADPH in insulin secretion. J Biol Chem 1995;270:20051-8.
[67] Xu J, Han J, Long YS, et al. Malic enzyme is present in mouse islets and modulates insulin secretion. Diabetologia 2008;51:2281-9.
[68] Li C, Nissim I, Chen P, et al. Elimination of KATP channels in mouse islets results in elevated [U-13C]glucose metabolism, glutaminolysis, and pyruvate cycling but a decreased {gamma}-aminobutyric acid shunt. J Biol Chem 2008;283:17238-49.